Plectin 1f scaffolding at the sarcolemma of dystrophic (*mdx*) muscle fibers through multiple interactions with β-dystroglycan

Günther A. Rezniczek,[1] Patryk Konieczny,[1] Branislav Nikolic,[1] Siegfried Reipert,[1] Doris Schneller,[1] Christina Abrahamsberg,[1] Kay E. Davies,[2] Steve J. Winder,[3] and Gerhard Wiche[1]

[1]Max F. Perutz Laboratories, Department of Molecular Cell Biology, University of Vienna, A-1030 Vienna, Austria
[2]Department of Physiology, Anatomy, and Genetics, Medical Reasearch Council Functional Genetics Unit, Oxford OX1 3QX, England, UK
[3]Centre for Developmental and Biomedical Genetics, Department of Biomedical Science, University of Sheffield, Western Bank, Sheffield S10 2TN, England, UK

In skeletal muscle, the cytolinker plectin is prominently expressed at Z-disks and the sarcolemma. Alternative splicing of plectin transcripts gives rise to more than eight protein isoforms differing only in small N-terminal sequences (5–180 residues), four of which (plectins 1, 1b, 1d, and 1f) are found at substantial levels in muscle tissue. Using plectin isoform–specific antibodies and isoform expression constructs, we show the differential regulation of plectin isoforms during myotube differentiation and their localization to different compartments of muscle fibers, identifying plectins 1 and 1f as sarcolemma-associated isoforms, whereas plectin 1d localizes exclusively to Z-disks. Coimmunoprecipitation and in vitro binding assays using recombinant protein fragments revealed the direct binding of plectin to dystrophin (utrophin) and β-dystroglycan, the key components of the dystrophin–glycoprotein complex. We propose a model in which plectin acts as a universal mediator of desmin intermediate filament anchorage at the sarcolemma and Z-disks. It also explains the plectin phenotype observed in dystrophic skeletal muscle of *mdx* mice and Duchenne muscular dystrophy patients.

Introduction

Transmission of force from skeletal muscle myofibrils to the ECM is thought to be mediated largely by intermediate filaments (IFs). Several IF proteins are expressed in muscle, including vimentin, nestin, synemin, syncoilin, lamins, cytokeratins, and desmin, the major muscle-specific IF protein (for review see Paulin and Li, 2004). The desmin IF network forms a 3D scaffold surrounding Z-disks, extends from one Z-disk to the next, and finally connects the contractile apparatus to the plasma membrane at the level of Z-disks but also to organelles such as mitochondria and the nucleus (for review see Capetanaki, 2002). The dystrophin–glycoprotein complex (DGC) has been implicated in mediating the IF-ECM link through syncoilin and synemin, which interact with desmin and bind to the DGC protein α-dystrobrevin (Bellin et al., 2001; Newey et al., 2001; Poon et al., 2002). The DGC is a large protein complex consisting of integral membrane proteins (α- and β-dystroglycan [βDG], α-, β-, γ-, and δ-sarcoglycan, and sarcospan), the >425-kD large actin-binding protein dystrophin, and dystrophin-associated proteins such as the syntrophins and α-dystrobrevin. Components of the DGC are part of the costameric protein network that, among other proteins, also includes integrins, vinculin, talin, α-actinin, and caveolin-3. Costameres are subsarcolemmal protein assemblies that circumferentially align in register with the Z-disks of peripheral myofibrils (for reviews see Spence et al., 2002; Ervasti, 2003); some authors include elements located above M-lines and in longitudinal lines in this term (Bloch et al., 2002).

Muscular dystrophies (MDs) are a group of clinically and genetically heterogeneous diseases characterized by progressive muscle wasting. Lack of dystrophin leads to the most common form, Duchenne MD (DMD), but MD can also result from mutations in genes whose products are not known to associate with the DGC (Burton and Davies, 2002). Most patients with plectin defects, who mainly suffer from various subtypes of the skin blistering disease epidermolysis bullosa (Pfendner et al., 2005), have also been diagnosed with MD, and muscle phenotypes have been observed in plectin-deficient mice (Andrä et al., 1997).

Correspondence to Gerhard Wiche: gerhard.wiche@univie.ac.at

Abbreviations used in this paper: ABD, actin-binding domain; βDG, β-dystroglycan; DGC, dystrophin–glycoprotein complex; DMD, Duchenne MD; EDL, extensor digitorum longus; IB, immunoblotting; IF, intermediate filament; IFM, immunofluorescence microscopy; IP, immunoprecipitation; MD, muscular dystrophy; MyHC, myosin heavy chain.

The online version of this article contains supplemental material.

The Journal of Cell Biology, Vol. 176, No. 7, March 26, 2007 965–977
http://www.jcb.org/cgi/doi/10.1083/jcb.200604179

The cytolinker protein plectin is prominently expressed in striated muscle cells and has been visualized at Z-disks, the sarcolemma, and at mitochondria (Wiche et al., 1983; Schröder et al., 1997; Reipert et al., 1999; Hijikata et al., 2003), but the molecular mechanisms involved in plectin-related muscle disease/defects are unknown.

Plectin is a large (M_r > 500,000) protein consisting of N- and C-terminal globular domains separated by an ~200-nm–long rod. The N-terminal domain contains a multifunctional actin-binding domain (ABD; Andrä et al., 1998) that is capable of also interacting with integrin β4 (Rezniczek et al., 1998; Geerts et al., 1999) and vimentin (Sevcik et al., 2004) and also contains binding sites for nesprin-3 (Wilhelmsen et al., 2005) and the nonreceptor tyrosine kinase Fer (Lunter and Wiche, 2002). The C-terminal domain contains binding sites for IFs (Nikolic et al., 1996), the γ1 subunit of AMP kinase (Gregor et al., 2006), and the PKC scaffolding protein RACK1 (Osmanagic-Myers and Wiche, 2004). Several different plectin isoforms, which are generated by tissue and cell type–dependent alternative splicing of transcripts from a single gene with >40 exons, form the basis for its broad versatility (Fuchs et al., 1999; Rezniczek et al., 2003). Isoforms with eight alternative N termini have been identified, and specific functions have been linked to distinct isoforms. Plectin 1a anchors keratin IFs to hemidesmosomes in basal keratinocytes (Andrä et al., 2003), and a specific role in fibroblast and T cell migration has been demonstrated for plectin 1 (Abrahamsberg et al., 2005).

In skeletal muscle, four isoforms (plectins 1, 1b, 1d, and 1f) are expressed at considerable levels. In this study, we address the following issues: Where on the subcellular level are these plectin isoforms localized in muscle fibers? What are their muscle-specific (novel) binding partners? Are they differentially regulated during differentiation? What role do they play in dystrophic muscle, such as that of *mdx* mice?

Results

Muscle fiber type–dependent expression and isoform-specific subcellular localization of plectin

Plectins 1d, 1f, 1b, and 1, the isoforms most abundantly expressed in skeletal muscle, show relative mRNA ratios of >10:4:3:1, respectively (Fuchs et al., 1999). To obtain data about their expression and localization in skeletal muscle on the protein level, we isolated the quadriceps, a typical fast-twitch muscle composed of mainly type 2 fibers, from 10-wk-old mice and processed it for immunolabeling. Anti–pan-plectin antiserum revealed strong subsarcolemmal and moderate sarcoplasmic staining in cross sections of small diameter fibers and only faint sarcoplasmic and sarcolemmal staining in larger diameter fibers (Fig. 1 C). On longitudinal sections, Z-disks were stained in all fibers, but the signal was much stronger in small diameter fibers, where additionally the plasma membrane was stained (Fig. 1 A). These fibers, which showed strong autofluorescence at 488 nm (Fig. 1, F and H; insets), were positive for myosin heavy chain (MyHC)–2A (Fig. 1 B; also see E, G, and I), whereas those with larger diameters were MyHC-2B positive (Fig. 1 K). Therefore, it appears that in quadriceps, fast 2A fibers express plectin at higher levels than type 2B fibers, as has previously been reported for type 2 compared with slow type 1 fibers (Schröder et al., 1997). Double immunolabeling of plectin 1f and MyHC-2A on longitudinal sections revealed this plectin isoform to be located at Z-disks in 2A fibers but to be hardly expressed in 2B fibers (Fig. 1, D and E; and not depicted). On cross sections, 2A fibers showed moderate sarcoplasmic plectin 1f–specific staining as well as irregular and weak staining of the membrane (Fig. 1, F and G). Staining of longitudinal sections using a plectin 1–specific antiserum revealed this isoform to be much less abundant, if at all present, at Z-disks. However, a strong

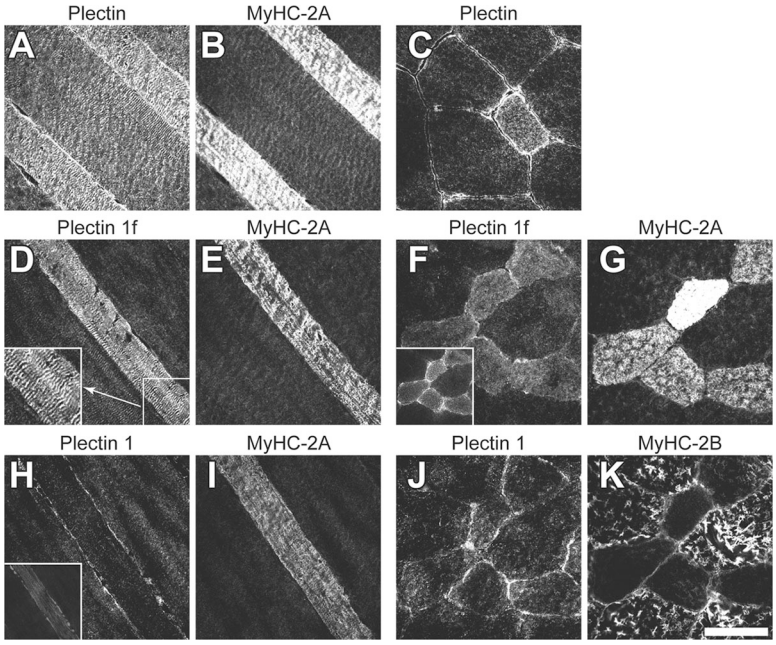

Figure 1. **Immunolocalization of plectin isoforms in quadriceps of 10-wk-old mice.** Consecutive (except A–C) serial longitudinal and cross sections were stained with antibodies (pan-plectin) recognizing all plectin isoforms (A and C) or specifically isoforms 1f (D and F) or 1 (H and J); in addition, antibodies specific to MyHC-2A (B, E, G, and I) and -2B (K), all in combination with Cy5-labeled secondary antibodies, were used. The boxed area in D (bottom right) is shown enlarged in the inset. The insets in F and H show autofluorescence after excitation at 488 nm recorded in the standard FITC channel. Bar, 50 μm.

signal came from sarcolemma-associated structures, primarily in 2A fibers (Fig. 1 H). On cross sections, plectin 1–specific signals were detected as irregularly distributed accumulations at the sarcolemma of 2A but not 2B fibers (Fig. 1 J).

As we were unsuccessful in generating isoform-specific antibodies directed against plectins 1b and 1d, we ectopically expressed and visualized GFP fusions of all four full-length plectin isoforms (1, 1b, 1d, and 1f) in myotubes (Fig. 2, A–D). Plectin 1 was expressed in a diffuse dotty pattern throughout the cytosol (Fig. 2 A; see virtual cross sections in insets 1 and 2) and was concentrated in the vicinity of nuclei. Immunolabeling with antibodies specific for sarcomeric α-actinin, a marker for Z-disks, revealed that areas positive for α-actinin were completely devoid of plectin 1 (Fig. 2 A, a and b; see areas marked by identically positioned arrowheads). Plectin 1b was distributed throughout the sarcoplasm in a pattern somewhat more patchy but similar to that observed for plectin 1, also mostly excluding areas that were positive for α-actinin (Fig. 2 B; a, b, and cross sections). Plectin 1d was located exclusively at structures identified as Z-disks (Fig. 2 C; arrowheads in a and b indicate the same exemplary positions). Contrary to expectations based on the immunostaining of tissue sections, plectin 1f was found not to be associated with Z-disks (Fig. 2 D). However, the observed sarcolemma association of this isoform was impressively confirmed (Fig. 2 D, virtual cross sections 1–4; a and b show individual confocal sections as indicated in panel 1). Immunolabeling of in vitro–differentiated C2C12 cells with plectin 1– and 1f–specific antibodies revealed the same localization of the native isoforms (unpublished data).

To further investigate the sarcolemma association of plectin, extensor digitorum longus (EDL) muscle was teased into single fibers, which were immunolabeled for plectin and βDG, a costameric membrane marker (Fig. 2 E). Both proteins colocalized in costameric structures. Whereas βDG staining resembled a gridlike pattern (Z-disks and longitudinal lines), pan-plectin serum revealed prominent Z-disk and perinuclear localization and only a rare association of plectin with longitudinal lines. Virtual cross and longitudinal sections (Fig. 2 E, insets 1 and 2) through confocal stacks showed plectin at the sarcolemma but also extending into the fibers in regular intervals. Analysis with isoform-specific antibodies showed distinct staining patterns for plectins 1 and 1f. Whereas plectin 1 was found in the perinuclear area, at longitudinal lines, and in a dotty pattern at Z-disks (Fig. 2 F), plectin 1f was strongly expressed at

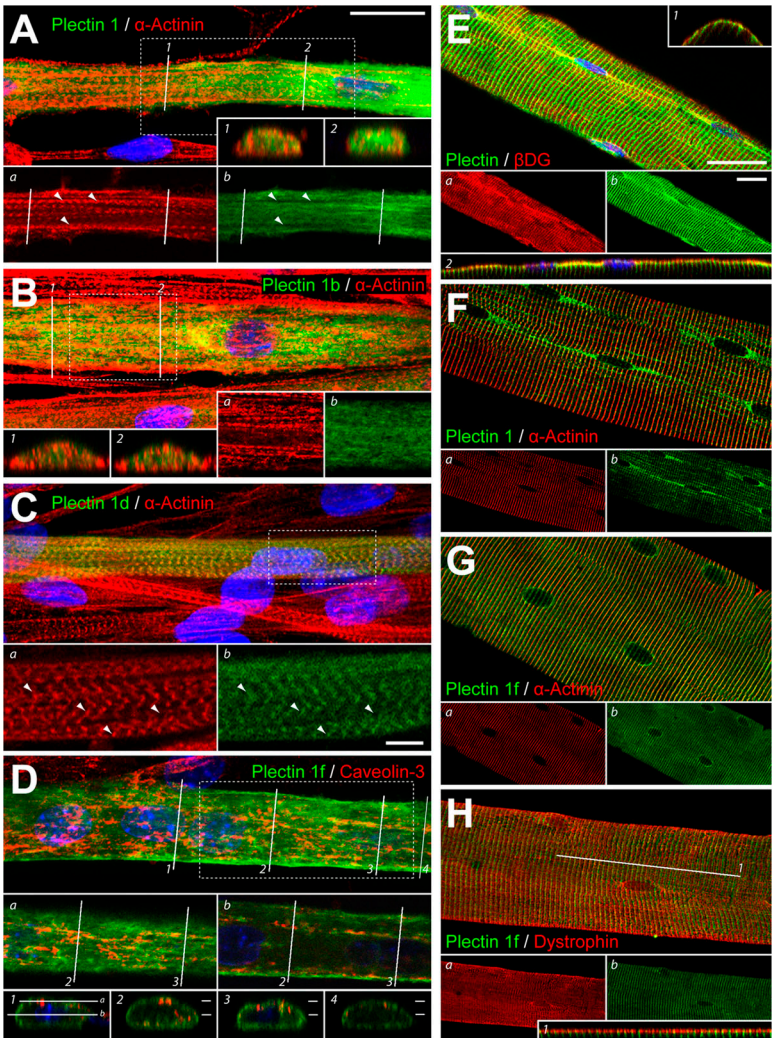

Figure 2. **Expression of full-length plectin isoforms in differentiated myotubes and immunostaining of teased muscle fibers.** (A–D) Full-length plectin 1 (A), 1b (B), 1d (C), or 1f (D) expression plasmids (with C-terminal EGFP; green) were transfected into myoblasts ~12–16 h before differentiation. After 96 h, differentiated myotubes were fixed with methanol and processed for immunolabeling using antibodies specific for sarcomeric α-actinin (A–C) or caveolin-3 (D). Secondary antibodies were Texas red labeled (red), and nuclei were visualized with Hoechst 33342 (blue). Main panels show composites of confocal stacks; dotted frames indicate areas shown in more detail in panels a and b of A–D. Numbered lines indicate confocal sections shown in correspondingly labeled insets; virtual cross sections were reconstructed from confocal stacks using LSM imaging software. Horizontal lines in insets 1–4 of D indicate the positions of the planes shown in panels a and b of D. Arrowheads in A and C indicate identical exemplary positions in panels a and b. (E–H) Teased fibers were prepared and processed for IFM as described in Materials and methods. Primary antibodies used were antiserum #123 to plectin (E), anti–plectin 1 (F), anti–plectin 1f (G and H), monoclonal anti-βDG (E), anti–α-actinin (F and G), and antidystrophin (H). Plectin-specific antibodies were detected with Cy3-conjugated secondary antibodies (green), and all others were detected with Cy5-conjugated secondary antibodies (red). Panels a and b show individual colors of the merged images. The virtual sections shown in insets 1 and 2 in E are from a different fiber. The line in H indicates the plane of section shown in inset 1. Bars in A and E apply to A–D and E–H, respectively; bars in panel b of C and E apply to panels a and b of A–D and E–H, respectively. Bars, 20 μm.

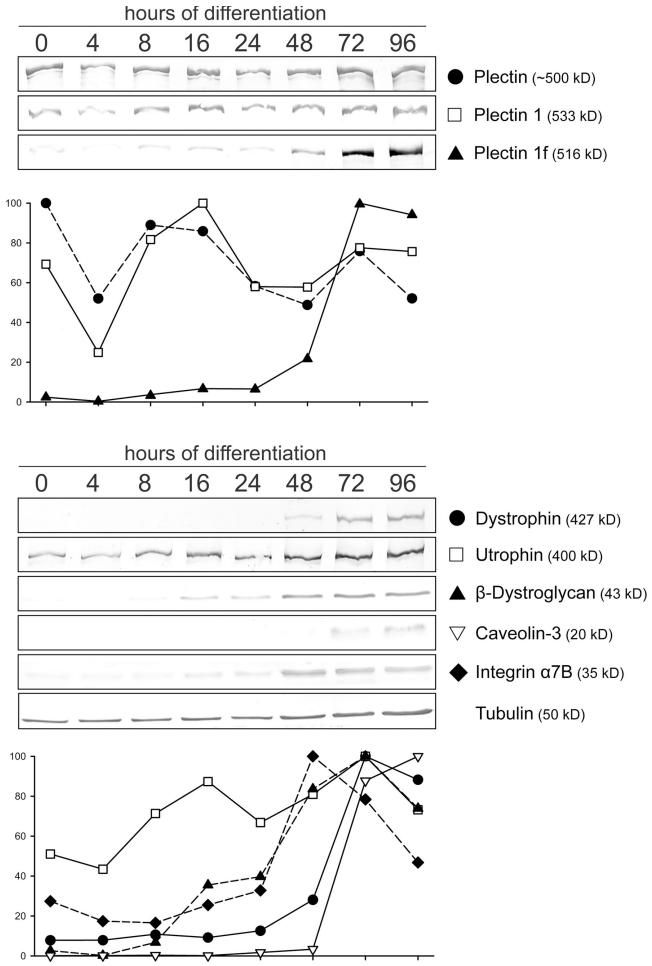

Figure 3. **Protein expression profiling during the differentiation of myoblasts in vitro.** Myoblasts isolated from plectin (+/+)/p53 (−/−) mice were differentiated in vitro for up to 96 h. Immediately before the start of differentiation and after 4, 8, 16, 24, 48, 72, and 96 h, cells were lysed in sample buffer, and proteins were separated by SDS-PAGE on 5% (plectin, dystrophin, and utrophin) or 15% (βDG, caveolin-3, integrin α7B, and tubulin) gels and analyzed by IB. Bands were scanned and evaluated densitometrically. Signals were normalized to tubulin and represent the means of at least triplicate experiments. 100% corresponds to the highest expression of each protein during the course of differentiation. Error bars (SD; rarely >10%) have been omitted for clarity.

Z-disks and tightly encircled nuclei (Fig. 2 G). Intriguingly, when the staining patterns for both isoforms are merged, they match that observed with pan-specific plectin antibodies, suggesting that plectins 1 and 1f are the major sarcolemma-associated isoforms. Costaining of plectin 1f with dystrophin revealed a partial colocalization of both proteins (Fig. 2 H). At the sarcolemma, plectin 1f was concentrated at Z-disks and extended into the fiber, whereas dystrophin was limited to the sarcolemma but was also found between Z-disks (Fig. 2 H, inset 1).

Coexpression of plectin 1f and dystrophin during myoblast differentiation

To define the role of plectin in the process of differentiation from myoblasts to myotubes, we profiled the expression of plectin and other skeletal muscle proteins (Fig. 3). After 96 h of differentiation, myoblast cultures had formed myotubes that started to twitch (unpublished data). During differentiation, plectin isoform 1 expression peaked at 8–16 h, which is similar to that of utrophin. Plectin 1f was expressed only later, starting between 24 and 48 h, and reached plateau levels after 72 h. Interestingly, dystrophin showed a very similar expression profile, whereas βDG was detectable earlier (16 h), and caveolin-3 was not detected before 48 h. Integrin α7B was already expressed in myoblasts and showed peak levels after ∼48 h of differentiation.

Plectin interacts with the EF-ZZ domains of dystrophin and utrophin

The spatially and temporally coordinated expression of plectin 1f and dystrophin suggested a possible direct interaction of both proteins. In immunoprecipitation (IP) experiments using IP lysates (see Materials and methods) from wild-type muscle tissue, plectin coprecipitated with dystrophin and vice versa (Fig. 4 A, lanes 5 and 7). From *mdx* IP lysates, which were used as negative controls, plectin was not precipitated using dystrophin antibodies (Fig. 4 A, lanes 6 and 8). Interestingly, although plectin was expressed at higher levels in *mdx* compared with wild-type muscles (Fig. 4 A, lanes 1 and 2), less of it was immunoprecipitated from *mdx* (Fig. 4 A, lanes 5 and 6; also see Fig. 6, A and C), indicating a shift of plectin into an insoluble pool. Utrophin and plectin were coprecipitated from rat fibroblast lysates (unpublished data). To identify interacting subdomains of the proteins, we immobilized His-tagged fragments of utrophin, including its N-terminal ABD, the C terminus, and the entire WW-ZZ domain as well as its three subdomains WW, EF, and ZZ on nitrocellulose membranes and overlaid them with various plectin samples (Fig. S1 A, available at http://www.jcb.org/cgi/content/full/jcb.200604179/DC1; summarized in Fig. 4 B). Using either purified full-length plectin or plectin-rich cell lysates, we found plectin bound to the ABD and WW-ZZ domain of utrophin but not to its C-terminal part. A recombinant plectin ABD showed similar specificity, although its binding to the utrophin ABD was very weak compared with that of full-length plectin. When overlaid onto WW-ZZ subdomains, positive signals were obtained for the EF and ZZ domains, whereas a fragment encoded by exons 9–12 of plectin did not show binding to any of the utrophin fragments used. Confirming these results, a Eu^{3+}-labeled version of the plectin ABD specifically bound to WW-ZZ domains of utrophin and dystrophin when overlaid onto microtiter plate–immobilized proteins (Fig. S1 B). Furthermore, the WW-ZZ domain of dystrophin competed with that of utrophin for plectin ABD binding as did actin (with considerably higher efficiency; Fig. S1 C). This suggested that simultaneous binding of actin and WW-ZZ domains to the plectin ABD was unlikely to occur.

Up-regulation of sarcolemmal plectin in *mdx* muscle

To define the relation of plectin with costameric membrane complexes in muscles lacking dystrophin, we characterized plectin localization in skeletal muscle fibers at different stages of MD in *mdx* mice by immunolabeling cross sections of quadriceps

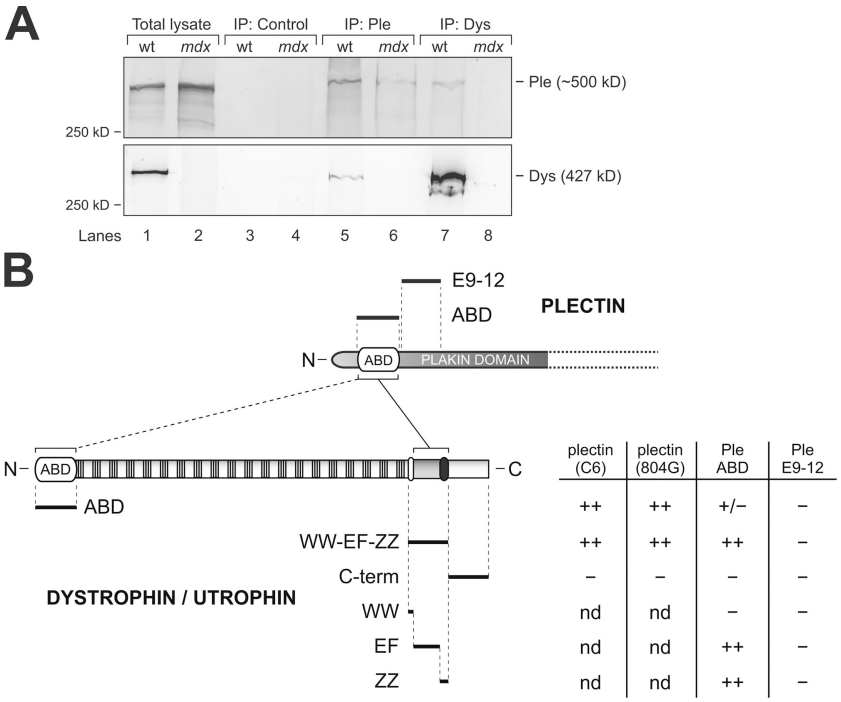

Figure 4. **Co-IP of plectin with dystrophin and direct binding of plectin to the utrophin/dystrophin EF-ZZ domain via its ABD.** (A) Total and IP lysates of wild-type (wt) and *mdx* muscle tissues were prepared as described in Materials and methods. IP lysates were incubated without (IP: Control) or with antibodies specific for plectin (IP: Ple) or dystrophin (IP: Dys). After separation and transfer to nitrocellulose, total lysates and precipitated samples were probed with antibodies specific for plectin (top) or dystrophin (bottom). (B) Schematic drawing of plectin and utrophin showing locations of binding interfaces, fragments used in blot overlay assays (bars above and below drawings), and a summary of binding data. Actual data are shown in Fig. S1 (available at http://www.jcb.org/cgi/content/full/jcb.200604179/DC1). N and C termini of proteins are indicated. ABD, actin-binding domain. Overlaid plectin was either purified from cell cultures (C6) or contained in cell lysates (804G). ++, strong binding; +/−, weak binding; −, no binding.

from 2-, 4-, and 14-wk-old animals with plectin-specific antibodies (Fig. 5, A–K). Compared with normal muscle, no differences were observed at the (prenecrotic) age of 2 wk (not depicted) and in unaffected areas of quadriceps from 4-wk-old (peak necrotic) *mdx* mice (Fig. 5, A and B and D and E). Plectin 1f was found in the sarcoplasm and irregularly at the sarcolemma, whereas plectin 1 was localized only in subsarcolemmal accumulations. Dystrophic areas were clearly distinguished by the presence of high numbers of small-diameter fibers with centralized nuclei and loose connective tissue, expressing very high levels of plectins 1 and 1f (Fig. 5, C and F). After 14 wk, most fibers had already passed through one round of degeneration/regeneration, and, as was expected from findings in DMD muscles (Schröder et al., 1997), we observed increased plectin staining at the sarcolemma of regenerated fibers when using a pan-plectin antibody (unpublished data). Isoform-specific antibodies revealed that this increased sarcolemmal staining was caused by the up-regulation of plectin 1f (Fig. 5, H and I vs. G). This was especially evident in 2B fibers, which are identified as large-diameter fibers lacking autofluorescence (Fig. 5 I; insets in G–I show autofluorescence). For plectin 1, on the other hand, we could not detect notable differences between *mdx* and control samples (Fig. 5, J and K). Thus, during the regeneration of *mdx* muscles, plectins 1 and 1f were both up-regulated in regenerating myotubes, but only plectin 1f associated with the sarcolemma and stayed there at high levels after regeneration was complete.

To obtain quantitative estimates of plectin up-regulation in *mdx* mice compared with other sarcolemma-associated proteins, we prepared KCl-washed microsomes from skeletal muscle of 8–10-wk-old *mdx* and control mice (Ohlendieck and Campbell, 1991; Cluchague et al., 2004). Compared with total muscle lysates (Fig. 6 A), microsome fractions from control muscle were enriched in DGC components (dystrophin, utrophin, and βDG) and the membrane markers caveolin-3 and integrin α7B; in addition, actin and plectins 1 and 1f but not tubulin were detected in microsomes (Fig. 6 B). Comparing corresponding control and *mdx* samples, we found increased levels of plectin (∼170%) and utrophin (∼140%) in total muscle lysates, whereas those of actin were similar (Fig. 6 C). Total plectin was two- to threefold more abundant in *mdx* versus control microsome fractions, with relative levels of plectin 1 and plectin 1f of ∼300% and ∼150%, respectively. Interestingly, the levels of utrophin in the sarcolemmal fraction were only ∼50% of those found in the wild type, suggesting a weaker membrane association of utrophin in *mdx* muscle. With our lysis protocol (see Materials and methods), the levels of βDG were found at ∼50% compared with the wild type, although *mdx* βDG levels as high as ∼100% of wild type have been reported when samples were treated with cholate detergent (Cluchague et al., 2004). Caveolin-3 appeared slightly increased, and no notable difference was observed in the case of actin. Interestingly, the *mdx* levels of integrin α7B were approximately fourfold increased (Fig. 6 D). Thus, these biochemical data were in agreement with the observed up-regulation of plectin in *mdx* muscle and the sarcolemma association of isoform 1f observed in the immunolabeling of tissue sections.

Utrophin is likely not the preferred binding partner of plectin at the sarcolemma of mature *mdx* muscle fibers

To assess whether utrophin was substituting for dystrophin as a linker protein between βDG and plectin in dystrophin-deficient muscle, we stained cross sections of *mdx* gastrocnemius for βDG and utrophin (Fig. 7, A–L). The antiserum to βDG gave a strong signal in control samples of all ages (2, 4, and 14 wk;

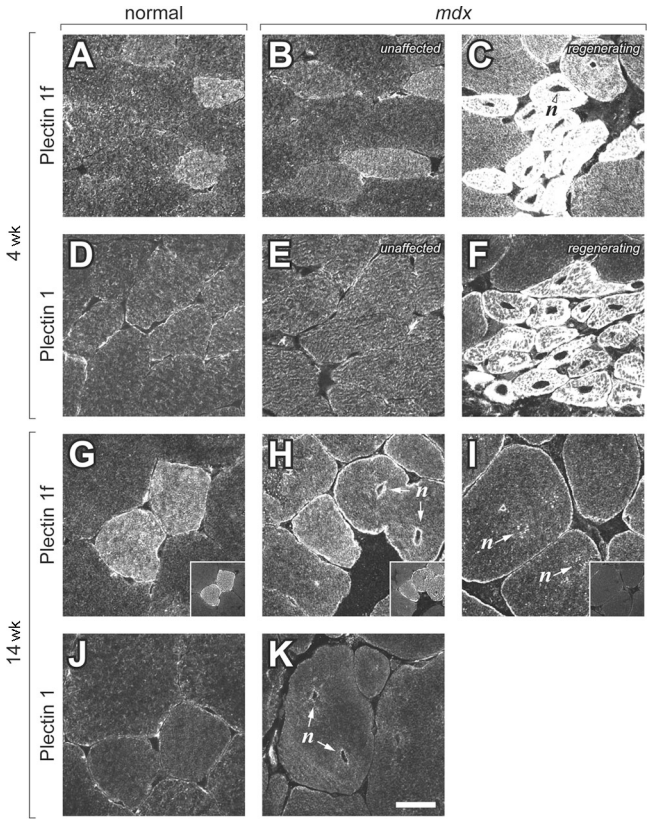

Figure 5. **Distribution of plectin isoforms 1 and 1f in muscle during the course of MD in *mdx* mice.** Cross sections of quadriceps from 4- and 14-wk-old *mdx* and normal control mice were immunolabeled with plectin 1f– (A–C and G–I) and plectin 1–specific antibodies (D–F, J, and K). Secondary antibodies used were Cy5 labeled. Areas of unaffected (B and E), actively regenerating (C and F), and regenerated (H, I, and K) *mdx* muscles are shown. Insets in G–I show autofluorescence after excitation at 488 nm, with autofluorescent fibers corresponding to type 2A fibers. *n*, sectioned nuclei. Bar, 20 μm.

Fig. 7, A, E, and I) and reduced but still clearly positive signals in the corresponding *mdx* samples (Fig. 7, C, G, and K). Actively regenerating *mdx* fibers, which are marked by small diameters and centralized nuclei, showed a much stronger staining at the age of 4 wk that was almost similar in intensity to the signal in control fibers (Fig. 7 G). Utrophin was strongly expressed at the sarcolemmas of 2-wk-old control animals, whereas only limited staining was observed in corresponding *mdx* muscle samples (Fig. 7, compare B with D). At later developmental stages of normal muscle, utrophin was detectable at myotendinous (Fig. 7 F, arrowheads) and neuromuscular junctions (not depicted), but no general sarcolemmal staining was observed (Fig. 7, F and J). In the case of 4- and 14-wk-old *mdx* muscle, utrophin was present exclusively in regenerating small-diameter fibers (Fig. 7, H and L; asterisks) and at myotendinous junctions (Fig. 7 H, arrowheads). Faint sarcolemmal utrophin-specific staining that was not visible in wild-type muscle was observed in *mdx* muscle (Fig. 7, H and L). The low levels of utrophin and the positive identification of βDG at the sarcolemma of *mdx* muscle prompted us to costain teased wild-type and *mdx* muscle fibers for plectin and βDG (Fig. 7, M–R). Both mAbs as well as an antiserum to βDG revealed that the gridlike staining pattern typical for costameres was lost in *mdx* fibers, and, instead, βDG was found exclusively above Z-disks together with plectin 1f (Fig. 7, compare the insets of N and P, which are magnified in Q and R). We also examined microsome fractions and sections prepared from muscles of *mdx*/utr$^{-/-}$ mice and found a similar situation as in *mdx* muscles (Fig. S2, available at http://www.jcb.org/cgi/content/full/jcb.200604179/DC1).

Direct interaction of plectin with βDG via multiple binding sites

The redistribution of βDG to sites above Z-disks where plectin 1f was concentrated suggested that plectin could directly interact with the cytoplasmic domain of βDG. Co-IP of both proteins from lysates of C2C12 myoblasts, mouse keratinocytes, and the human colon adenocarcinoma cell line CaCo-2 using anti-βDG antibodies was successful (Fig. 8 A). Using no or irrelevant antibodies, neither plectin nor βDG was detectable in the corresponding precipitates (unpublished data). Plectin and βDG could also be coprecipitated from lysates of skeletal muscle from *mdx* mice (Fig. 8 B). Immuno-EM confirmed the close association of both proteins at the sarcolemma of muscle fibers (Fig. 8 C). When the plasma membrane was lost as a result of Triton X-100 extraction, βDG remained anchored to subsarcolemmal filamentous structures (Fig. 8, white arrowheads), which were also positive for plectin (Fig. 8 D). βDG and plectin labeling was most prominent at subsarcolemmal regions overlying Z-disks. Additionally, the plectin label was concentrated at the periphery of Z-disks (Fig. 8 E).

To map the βDG-binding sites on plectin, a panel of His-tagged plectin fragments representing different structural domains (Fig. 9, A and B) were blotted onto nitrocellulose and overlaid with the cytoplasmic domain of βDG. The WW-ZZ domain of dystrophin, which binds to the C terminus of βDG (Ilsley et al., 2002), and the utrophin ABD or BSA were used as positive and negative controls, respectively. Using βDG-specific antibodies for detection, we found an interaction of βDG with two nonoverlapping plectin fragments (Fig. 9 C). One was encoded by plectin exons 12–24, representing part of the plakin domain located C terminally of the ABD within the plectin N-terminal globular domain, and the other corresponded to the C terminus of plectin, starting within repeat domain 4. No other protein tested showed binding except for the dystrophin WW-ZZ domain. To narrow down the region of βDG involved in binding to plectin, a fragment (βDGcytΔDBS) corresponding to roughly 70% of the βDG cytoplasmic domain (lacking the C-terminal region containing the dystrophin/utrophin-binding motif) was overlaid onto the same panel of recombinant proteins (Fig. 9 D). It bound to both plectin fragments identified before but bound much weaker to the C-terminal plectin fragment (Ple R_4-C), suggesting that additional C-terminal βDG sequences were needed for efficient binding to this fragment. As expected, the truncated βDG fragment failed to bind to the dystrophin WW-ZZ domain.

Binding of βDG to both plectin fragments was efficiently blocked by the dystrophin WW-ZZ domain (Fig. 9 E). When dystrophin was added to the overlay solutions at an equimolar ratio, βDG–plectin binding was only slightly reduced, but

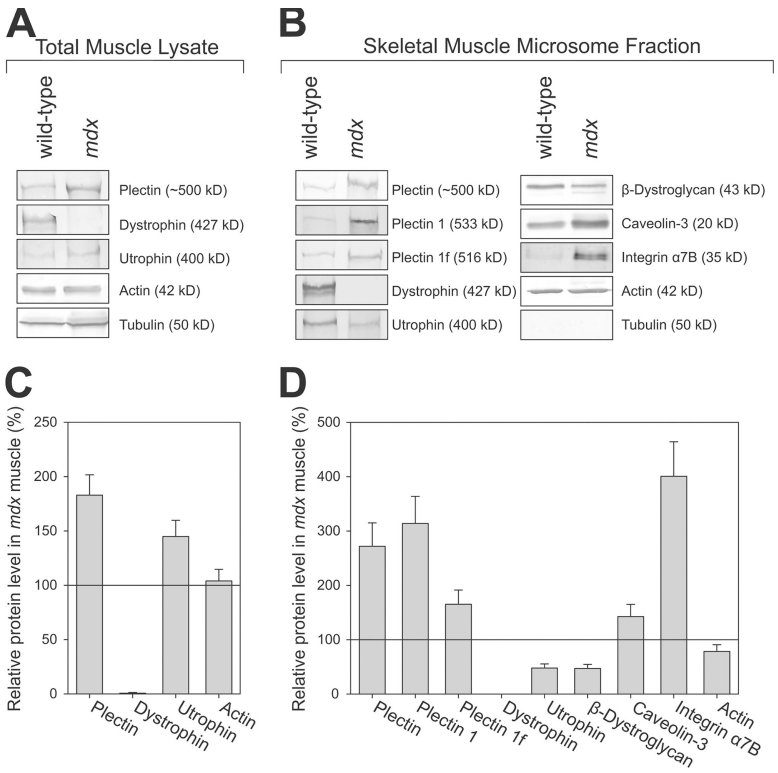

Figure 6. **Comparative (semiquantitative) IB analysis of total cell lysates and microsome fractions from control and *mdx* skeletal muscles.** (A and B) Scans of typical bands obtained by IB. (C and D) Bands were evaluated as described in Fig. 3. Signals were normalized to tubulin (total lysates) or total protein content (microsome fractions) and are shown relative to protein amounts in control (wild type) samples (100%). Values represent means ± SD (error bars) of at least three gel runs using samples from two independent preparations.

increasing the molar ratios to 1:5 or 1:10 in favor of dystrophin led to strongly reduced binding and no binding, respectively. Unexpectedly, in this competition experiment, positive signals were observed in two additional lanes (Ple E1–12 and Utr ABD; Fig. 9 E), suggesting that the dystrophin WW-ZZ domain mediated the indirect binding of βDG to the ABDs of utrophin

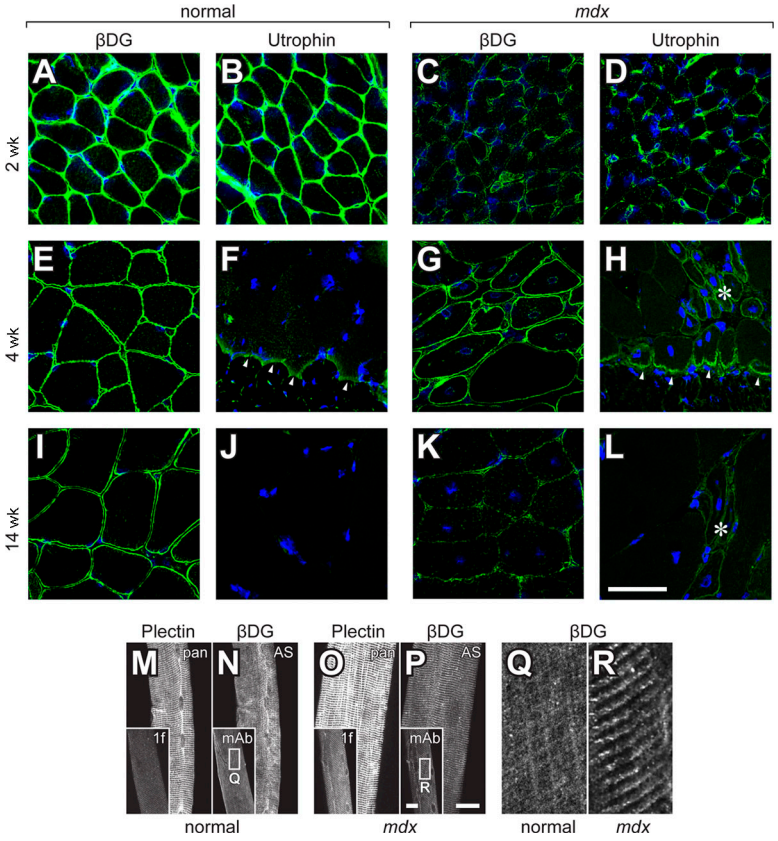

Figure 7. **Expression of βDG and utrophin during the course of MD in *mdx* mice and localization of βDG in teased muscle fibers.** (A–L) Cross sections of gastrocnemius from 2-, 4-, and 14-wk-old normal control (A, B, E, F, I, and J) and *mdx* (C, D, G, H, K, and L) mice were immunolabeled using antibodies specific for βDG (A, C, E, G, I, and K) and utrophin (B, D, F, H, J, and L). Note the expression (albeit reduced at ages 2 and 14 wk) of βDG in *mdx* muscle fibers. Utrophin is present at the sarcolemma of muscle fibers from young (<4 wk old) animals (normal and *mdx*) as well as in regenerating fibers from adolescent and adult *mdx* animals; at these stages, utrophin localization in nonregenerating fibers is virtually confined to myotendinous junctions both in normal and *mdx* mice (arrowheads in F and H). Asterisks in H and L denote areas of active regeneration in *mdx* muscle. (M–R) Teased fibers from normal and *mdx* muscles from 8-wk-old mice were stained with pan-plectin mouse antiserum #123 (pan), rabbit antiserum to plectin 1f (insets) and rabbit antiserum #1710 (AS), or mouse mAbs (insets) to βDG. Control and *mdx* samples were stained in parallel, and images were recorded using the same settings. Q and R show magnifications of the areas labeled Q and R in the insets in N and P. Bars (A–L), 50 μm; (M–P) 20 μm.

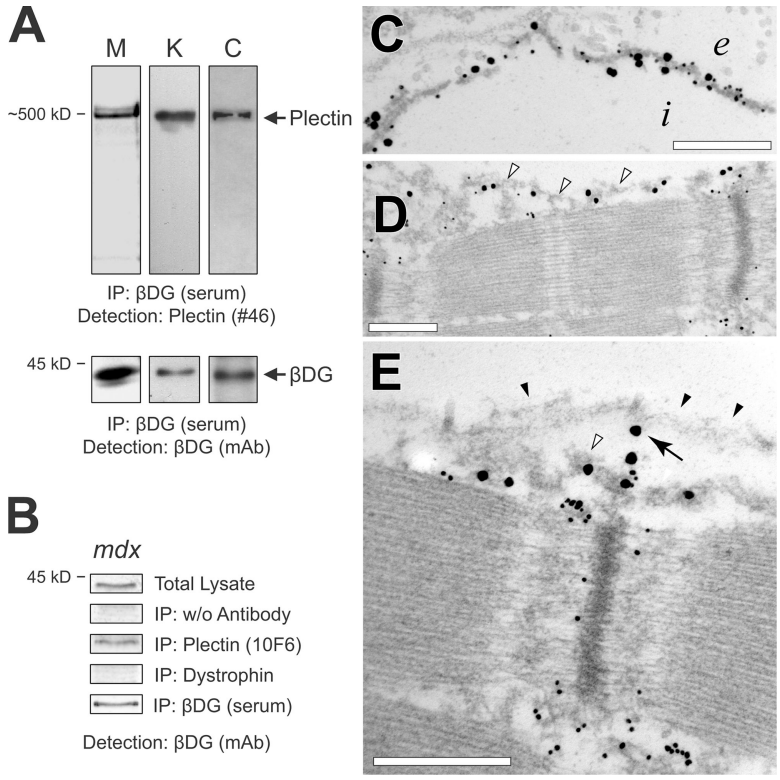

Figure 8. **Co-IP and ultrastructural colocalization of plectin and βDG.** (A) Cell lysates from C2C12 myoblasts (M), mouse keratinocytes (K), and CaCo-2 (C) cells were subjected to IP using anti-βDG antiserum; antibodies used for detection are indicated. (B) *mdx* muscle lysates were immunoprecipitated with the indicated antibodies and probed for βDG. (C–E) Preembedding immunogold labeling of teased muscle fibers extracted with Triton X-100. Gold particles labeling plectin (5 nm) and βDG (10 nm) were silver enhanced. In C, note the intense labeling of both proteins at the plasma membrane locally separated from the muscle fiber. The exterior of the fiber (e) contains extracellular material, whereas the blistered interior (i) is empty. In D, a sarcomere positioned beneath the sarcolemma is shown. Although the plasma membrane is lost by Triton X-100 extraction, βDG as well as plectin remain anchored to filamentous structures (arrowheads) in the subsarcolemmal region. Also note plectin labeling in the interior of the fiber at Z-disks. In E, details of a sarcomeric region proximal to a Z-disk are shown. Labeling of βDG is restricted to the subsarcolemmal region with incomplete detachment of the sarcolemma. While most of the βDG is located at filamentous structures (white arrowheads), it can also be observed (arrow) in association with the sarcolemma (black arrowheads). Bars, 500 nm.

and plectin. To confirm the simultaneous binding of WW-ZZ domains to plectin and βDG, we performed an overlay assay in which the utrophin WW-ZZ domain was immobilized on microtiter plates and incubated with constant amounts of Eu^{3+}-labeled βDG in the presence of increasing concentrations of labeled or unlabeled versions of the plectin ABD (Fig. 9 F). In the first case, the amounts of labeled protein bound remained unchanged (Fig. 9 F, gray bars), whereas signals were additive (Fig. 9 F, black bars) in the latter, clearly demonstrating that plectin and βDG bound to independent binding sites within the WW-ZZ domain.

Discussion

Distinct regulation and localization of plectin isoforms in skeletal muscle

Muscle formation is an incremental process in which differentiating myoblasts fuse and form primary and finally secondary myotubes. As this process involves massive rearrangements of the cytoskeleton, it was not unexpected to find that plectin isoforms were differentially expressed during its course. Of special interest was the striking similarity of the temporal expression patterns of plectin 1f and dystrophin, which suggested a role for this particular plectin isoform in the formation and maturation of costameres. This is supported by the observed exclusive membrane association of a recombinant version of this isoform in differentiated myotubes but not at the myoblast stage, where dystrophin is absent. A similar role of plectin had been suggested previously by Schröder et al. (2000, 2002), who concluded from their myoblast differentiation experiments that the association of plectin with Z-disks is a prerequisite for formation of the intermyofibrillar desmin cytoskeleton and, furthermore, that plectin is a component of primary longitudinal adhesion structures, which are precursors of costameres that form mature costameres only after being subjected to contractile forces. This would also explain the apparent discrepancy in plectin 1f localization in the tissue and in teased fibers (sarcolemma and Z-disks) versus transfected myotubes (sarcolemma only), as the latter represent a less mature stage. Interestingly, using mAb 121 to plectin, Schröder et al. (2002) identified a membrane-associated plectin variant that is up-regulated during human myotube differentiation. Our results would suggest that this variant is plectin 1f. However, it is unexplainable how a mAb with an epitope in plectin's rod domain could specifically detect one rod-containing isoform (1f) over others.

Immunostaining of muscle tissue revealed that plectin expression levels in individual fibers varied and were dependent on the fiber type. In cross sections of normal striated human muscle, a moderate to intense cytoplasmic and sarcolemmal staining of plectin has been reported in type 1 (slow twitch) fibers, whereas only faint staining of the sarcolemma was observed in type 2 (fast twitch) fibers (Schröder et al., 1997). In the present study, we show using an antiserum to plectin not discriminating among isoforms that in quadriceps (a typical fast muscle composed of mainly type 2 fibers), plectin clearly was localized at Z-disks in both type 2A and 2B fibers, with a stronger signal in 2A fibers. This corresponds well with the intense staining obtained with plectin 1f–specific antibodies in this fiber type. Neither with anti–plectin 1f nor anti–plectin 1 antibodies did we detect substantial Z-disk staining in 2B fibers. Based on this observation, one other plectin isoform expressed in skeletal muscle, plectin 1b or 1d, must be associated

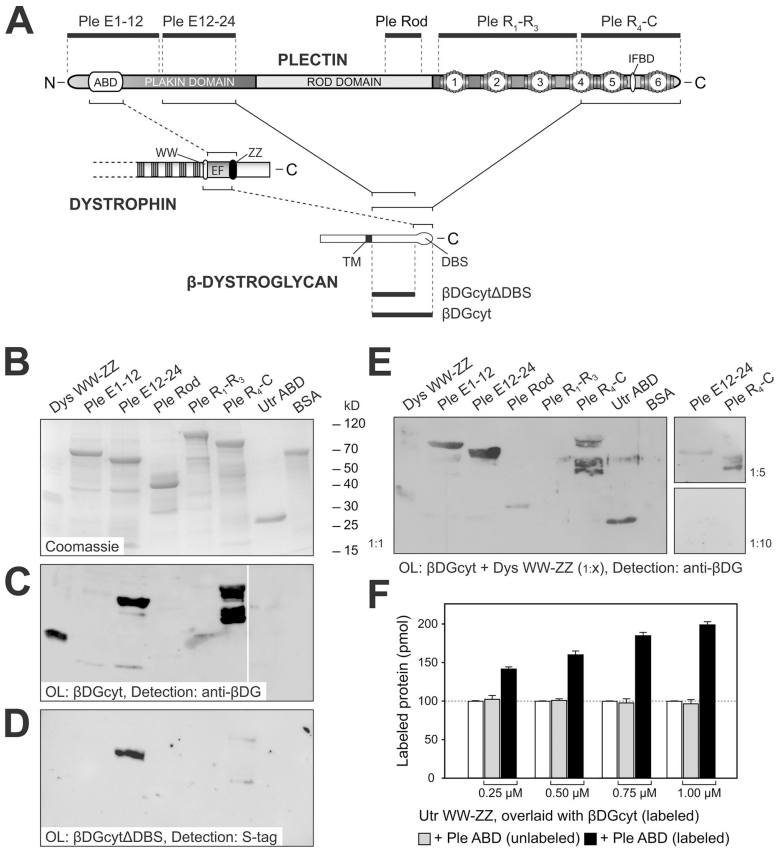

Figure 9. **Direct binding of βDG to N- and C-terminal domains of plectin.** (A) Schematic representation of plectin, βDG, dystrophin, and protein fragments used for in vitro interaction assays. Binding interfaces between plectin, dystrophin, and βDG are indicated by brackets connected by lines. ABD, actin-binding domain; IFBD, IF-binding domain; TM, transmembrane domain; DBS, dystrophin-binding site. N and C termini of proteins are indicated. (B–E) Blot overlay assay. A panel of protein fragments recombinantly expressed in bacteria (B; Coomassie) was immobilized on nitrocellulose membranes and overlaid with βDGcyt (C) or βDGcytΔDBS, a shorter fragment comprising amino acids 765–857 and lacking the dystrophin-binding site (D). Bound proteins were detected using mAbs to βDG (C) or via the S tag contained in βDGcytΔDBS (D). In E, membranes were overlaid with βDGcyt in the presence of Dys WW-ZZ, a fragment corresponding to the WW-ZZ domain of dystrophin. Molar ratios (βDGcyt/Dys WW-ZZ) were 1:1, 1:5, and 1:10 in the large, small top, and small bottom panels, respectively. (F) Microtiter plate competition binding assay. Recombinantly expressed and purified WW-ZZ domains of utrophin (immobilized) were overlaid with constant amounts of a Eu^{3+}-labeled version of the full-length cytoplasmic domain of βDG (βDGcyt; white bars; 100% indicated by the dotted line) and increasing amounts of unlabeled (gray bars) or Eu^{3+}-labeled (black bars) recombinant plectin ABD. Data represent mean ± SD (error bars) of a typical experiment performed with triplicate wells.

with Z-disks in type 2B fibers. From our overexpression experiments, we conclude that this isoform is plectin 1d, as it was found localized exclusively at Z-disks. At this time, the molecular mechanism of this targeting is unknown.

Plectin is associated with the DGC via multiple interfaces

Using co-IP and in vitro binding assays, we demonstrate direct interactions of plectin via multiple interfaces with components of the DGC, including (1) direct binding of its plakin domain to the cytoplasmic domain of βDG; (2) direct binding of its C-terminal portion to βDG; (3) binding of its ABD to the WW-ZZ domains of dystrophin and utrophin; and (4) binding of its ABD to the ABD of utrophin (Figs. 4 and 9, schematics). Whether the ABD of plectin would also interact with that of dystrophin remains an open question considering that the functionalities of the ABDs of dystrophin and utrophin differ (Rybakova et al., 2006), whereas their WW-ZZ domains are highly conserved (Hnia et al., 2007). Plectin and dystrophin had previously been coimmunoprecipitated from muscle lysates, but their interaction was assumed to be indirect via actin (Hijikata et al., 2003). In dystrophin-lacking *mdx* mice, one may thus expect to find the reduced sarcolemma association of plectin, but our immunofluorescence and tissue fractionation experiments revealed that plectin was instead enriched at the sarcolemma of *mdx* muscle. It was widely believed that dystrophin deficiency in skeletal muscles of *mdx* mice and DMD patients leads to the reduced expression and sarcolemmal association of dystrophin-associated proteins, including a strong reduction or even absence of βDG immunoreactivity (Ohlendieck and Campbell, 1991) despite its mRNA levels being similar to those in normal samples (Ibraghimov-Beskrovnaya et al., 1992; Rouger et al., 2002). However, in a recent study, Cluchague et al. (2004) challenged this view when they demonstrated that in *mdx* muscle samples treated with 2% cholate, βDG was detectable at levels comparable with those of wild-type samples. The authors proposed that βDG was targeted to the plasma membrane normally in dystrophin-deficient *mdx* muscles but remained inaccessible to antibodies and, when tissues were lysed, became part of an SDS-insoluble pool. Using our protocols, we also found considerable levels of βDG in *mdx* skeletal muscle microsome fractions (~50% of wild type even without cholate treatment), and we were able to immunodetect βDG with variable intensities throughout *mdx* muscle regeneration. Thus, our results support the hypothesis of Cluchague et al. (2004), and the direct interaction of plectin with βDG provides an explanation for the observed increase in sarcolemmal plectin in *mdx* muscle (Fig. 10). In the absence of dystrophin, more plectin can bind to βDG, causing at the same time the redistribution and accumulation of βDG above Z-disks, where plectin is normally localized. Matching our βDG immunostaining results, Yurchenco et al. (2004) have observed a corresponding redistribution of αDG in teased *mdx* fibers.

It has been suggested that utrophin could substitute for dystrophin in dystrophic muscles, but its intimate association with βDG may be limited to the time of regeneration only (Tinsley et al., 1998). The ~50% reduction of utrophin observed in

microsome preparations from muscle of ~10-wk-old *mdx* mice despite the overall higher expression of utrophin (~150% of wild-type levels) would support this notion. Furthermore, this observation also suggests that plectin binds to βDG with a higher affinity than utrophin. Remaining sarcolemmal utrophin staining that was observed in transgenic *mdx* mice overexpressing Dp71, a short splice variant of dystrophin lacking rod and N-terminal domains (Cox et al., 1994; Greenberg et al., 1994), was explained by Cox et al. (1994) to possibly be caused by the binding of utrophin to subsarcolemmal actin via its ABD. Our finding that βDG immunostaining signals observed in *mdx* tissue from 4-wk-old animals was almost as strong as in normal muscle would also fit the proposed model (Fig. 10), as the higher expression of utrophin during the phase of peak necrosis/regeneration may displace plectin from βDG and, thus, restore accessibility of the epitopes masked by plectin. Similarly, the overexpression of Dp71 (or other dystrophin or utrophin deletion variants) in *mdx* restored normal DGC components, whereas a full phenotypic rescue was achieved only by proteins with functional ABDs and intact C-terminal βDG-binding domains (Tinsley et al., 1998).

Plectin acts as a universal mediator of IF anchorage

The DGC has been considered to be responsible for connecting the subsarcolemmal actin cytoskeleton to the ECM, and disruption of this link causes a dystrophic phenotype. However, in recent years, it has been established that the contractile actions of a muscle fiber are mechanically integrated by desmin IFs, which are responsible for linking individual myofibrils laterally with each other and to the sarcolemma at the level of the Z-disks. Previous studies have implicated the DGC as the transmembrane complex linking the IF network with the ECM (for reviews see Blake and Martin-Rendon, 2002; Capetanaki, 2002; Paulin and Li, 2004). The necessary link would be created by an α-dystrobrevin–synemin/syncoilin–desmin bridge. Synemin may also directly interact with vinculin, providing an alternative anchorage of desmin IFs to costameres (Bellin et al., 2001). Plectin directly interacts with desmin via its C-terminal IF-binding domain (Reipert et al., 1999) and also with multiple components of the DGC, including its transmembrane core protein βDG. Thus, we propose that plectin acts as a direct linker between the DGC and the desmin IF network. There is precedence for such a function of plectin in basal keratinocytes, where the protein directly links the keratin IF network to the cytoplasmic domain of the β subunit of the laminin receptor integrin α6β4 (Rezniczek et al., 1998). It could be that synemin plays the essential role in establishing the direct linkages between heteropolymeric IFs and the myofibrillar Z-disk and costameric regions, and plectin might only provide additional structural support at these sites. However, this would be in conflict with observations in differentiating human skeletal muscle cultures, where plectin was already localized in a cross-striated pattern, whereas desmin was still found in longitudinal filaments (Schröder et al., 2000).

Recently, it was shown that besides type III and IV IFs, the cytokeratins K8 and K19 are also expressed in striated muscle and localize to Z-disks and M-lines and that K19 directly

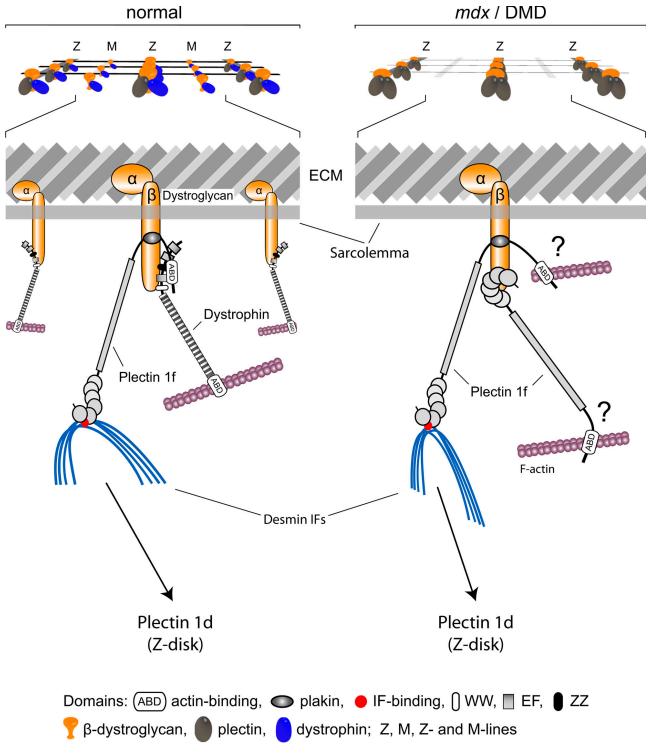

Figure 10. **Model of DGC-cytoskeleton linkage via plectin in normal and *mdx*/DMD muscle fibers.** Under normal conditions (left), plectin molecules are associated with the DGC by binding to βDG via the binding site in its plakin domain and/or by binding to dystrophin via its ABD, leaving the IF-binding domain available for binding to the desmin IF network. Binding of dystrophin and plectin to βDG may occur simultaneously at costameric structures above Z-disks but not M-lines (smaller-scale structures). When dystrophin is absent (right), plectin can additionally bind with its C-terminal domain to βDG using a binding site on βDG normally occupied by dystrophin. This leads to increased levels of plectin at the sarcolemma and to a redistribution of βDG (and DGCs) from their normal gridlike localization (top left) to areas overlying Z-disks only (top right). Furthermore, the tight interaction with multiple plectin molecules causes the complex to become SDS insoluble (see Discussion). Binding to βDG via the C-terminal domain could leave the plectin ABD available for binding to filamentous actin, potentially fulfilling to some degree dystrophin's function of linking the DGC to the actin cytoskeleton. However, the ABD of plectin and potentially also signaling molecules scaffolded on plectin may have adverse regulatory effects.

interacts with the dystrophin ABD (Stone et al., 2005). Whereas plectin has been shown to directly bind to keratins 5, 14, and 18 (Geerts et al., 1999; Steinböck et al., 2000), it is unknown whether it can also interact with the muscle-specific keratins and possibly plays a role in their anchorage as well.

Based on our observations, we propose the following model for plectin's association with the DGC (Fig. 10). Because (1) binding of plectin to βDG via its C-terminal binding site was abolished in the absence of the C-terminal part of βDG's cytoplasmic domain (harboring the PPxY motif required for interaction with the WW domain of dystrophin and utrophin; see Ilsley et al., 2002 for a discussion of the WW domain and its interactions) and (2) binding of plectin to βDG was efficiently blocked by dystrophin, only a portion of the βDG cytoplasmic tails would normally be available for binding to plectin when dystrophin is present. However, plectin could remain associated with the DGC via binding of its ABD to dystrophin (utrophin).

In such a constellation, the plectin C-terminal domain, separated from the N terminus by the ~200-nm–long rod domain, would be exposed and available for binding to muscle IFs (desmin and potentially also cytokeratins 8/19). In the absence of dystrophin, however, the available binding sites on βDG are occupied by plectin, leading to the increased sarcolemmal plectin 1f signal observed in *mdx*, *mdx*/utr$^{-/-}$, and DMD muscle fibers and consequently to an increased insolubility of βDG and masking of its epitopes. Binding via the C terminus would also leave the plectin ABD available for interaction with filamentous actin, possibly taking over some of the responsibilities of dystrophin. Finally, based on the cellular targeting of overexpressed recombinant full-length versions of plectin isoforms, we propose plectin isoform 1d to be involved in the anchorage of desmin IFs to Z-disks (Fig. 10, bottom).

DGC signaling: plectin as a scaffold?

Recently, several proteins involved in signaling such as nonreceptor tyrosine kinase Fer, the PKC scaffolding protein RACK1, and the key enzyme involved in energy homeostasis, AMP kinase, have been identified as novel interaction partners of plectin and led to the proposal that plectin acts as a scaffolding platform for signaling proteins in addition to serving as a cytoskeletal linker. Having established plectin as a component of the DGC with multiple binding interfaces to its key components, it will now be a challenge to define its role in DGC-mediated signaling. An important consequence implied by our model could be that misguided signaling mediated by the accumulation of plectin scaffolds at the sarcolemma of *mdx* and DMD dystrophic muscle contributes to the disease phenotype.

Materials and methods

cDNA constructs

Full-length (mouse) plectin isoform cDNA constructs (including respective 5′ untranslated regions) encoding proteins with C-terminal GFP have been described previously (Rezniczek et al., 2003). For bacterial expression of plectin fragments, the corresponding cDNAs were PCR amplified by using primers with EcoRI tails and were cloned into pJD1, a modified pET-15b (Novagen) that was obtained by replacing the EcoRI–BamHI fragment of pBN120 with that from pAD29 (Nikolic et al., 1996); expressed proteins contained an N-terminal His tag and a C-terminal *c-myc* tag. The following plectin fragments were used: Ple E1–12 (M_1–R_{654}), Ple E9–12 (E_{419}–V_{541}), Ple E12–24 (M_{546}–E_{1128}), Ple Rod (E_{2235}–Q_{2577}), Ple R_1–R_3 (A_{2762}–K_{3852}), and Ple R_4–C (L_{3850}–A_{4687}), which were all from a rat (X59601), as well as Ple ABD (D_{181}–N_{418}) from a mouse (NM_201389). To express N-terminally His-tagged versions of human utrophin (X69086) fragments, Utr ABD (S_{19}–D_{261}), Utr WW-ZZ (A_{2798}–M_{3113}), Utr WW (A_{2798}–K_{2868}), Utr EF (I_{2869}–S_{3014}), Utr ZZ (N_{3015}–M_{3113}), and Utr C-terminal (M_{3204}–M_{3433}) EcoRI-flanked cDNAs were cloned into pBN120 (Nikolic et al., 1996). The WW-ZZ domain (A_{3041}–M_{3356}) of human dystrophin (X14298) was also expressed from pBN120. Fragments βDGcyt (L_{765}–P_{895}) and βDGcytΔDBD (L_{765}–D_{857}) of human βDG (NM_004393) were expressed from pIJ1 (a pET32a [Novagen]-derived plasmid in which the sequence between the NcoI and XhoI restriction sites has been replaced by 5′-AATTCCTGGTGCCACGCGGTTCT-3′) as proteins with N-terminal Trx-His-S tags and C-terminal His tags. The cDNA fragments encoding Ple ABD and Dys WW-ZZ were also inserted into the EcoRI site of pMal-c2 (New England Biolabs, Inc.) to generate fusion proteins with N-terminal maltose-binding protein.

Antibodies

For immunoblotting (IB), IP, immunofluorescence microscopy (IFM), and immuno-EM, the following antibodies were used: mAbs 5B3 (IB) and 7A8 (EM; Rezniczek et al., 2004) to plectin; antisera #9 (IB), #46 (IFM), and #123 (IFM) to plectin (Andrä et al., 2003); anti–plectin isoform 1 antiserum (IB and IFM; Abrahamsberg et al., 2005); anti–plectin isoform 1f antiserum (IB and IFM), which was prepared and affinity purified as described previously (Abrahamsberg et al., 2005) using amino acids M_1–K_{28} of plectin 1f (NM_212539) as immunogen; mAb EA-53 (Sigma-Aldrich) to sarcomeric α-actinin (IFM); mAb AC-40 (Sigma-Aldrich) to actin (IB); mAb B-5-1-2 (Sigma-Aldrich) to tubulin (IB); mAb 43DAG1/8D5 (IB, IFM, and IP; Novocastra) and rabbit antisera #1709 and #1710 (Tyr 895-P; IB, IFM, IP, and EM; Ilsley et al., 2001) to βDG; anti-utrophin antiserum RAB5 (IB, IP, and IFM; James et al., 2000); mAb DY4/6D3 (Novocastra) to dystrophin (IB); mAb (clone 26) to caveolin-3 (IB and IFM; BD Biosciences); anti–integrin α7 antiserum (IB; provided by U. Mayer, University of East Anglia, Norwich, UK; Cohn et al., 1999); mAbs to MyHC-2A (SC-71) and -2B (BF-F3; IFM; hybridomas were obtained from the German Resource Center for Biological Material; Schiaffino et al., 1989); and mAb to myc epitope tag (1-9E10.2; IB; American Type Culture Collection). As secondary antibodies, we used goat anti–rabbit IgG AlexaFluor488 (Invitrogen), goat anti–mouse IgG Texas red (Jackson ImmunoResearch Laboratories), and donkey anti–rabbit Cy5 (Jackson ImmunoResearch Laboratories) for IFM and used goat anti–rabbit and goat anti–mouse IgGs conjugated to AP or HRP (Jackson ImmunoResearch Laboratories) for IB.

Immunocytochemistry

Thin sections (3–5 μm for longitudinal and 8–10 μm for cross sections) were prepared from skeletal muscle (quadriceps and gastrocnemius) dissected from C57BL/10 control and *mdx* mice (Institut für Labortierkunde, Medical University of Vienna) and frozen in liquid nitrogen–cooled isopentane. Sections were placed on slides, fixed with acetone for 10 min, and incubated for 1 h in 5% goat serum in PBS to block nonspecific binding of antibodies. Samples were incubated with primary and secondary antibodies diluted in PBS for 1 h each. Signal specificity was controlled by the omission of primary antibodies or by using normal mouse or rabbit serum in their place. To prepare teased fibers, mice were anesthetized with isoflurane and perfused with 2% PFA in PBS. EDL was dissected and incubated with the same fixing solution for 10 min. Using fine forceps, the muscle was teased into single fibers, which were then adhered onto chrome-alaun/gelatin-coated slides. Slides were blocked with PBS containing 0.1% BSA and 0.1% Triton X-100 for 1 h, incubated for 2 h with primary antibodies (diluted in blocking solution), washed with PBS for 30 min, incubated with secondary antibodies (diluted in PBS) for 1.5 h, and washed again with PBS. Finally, samples were briefly rinsed with water and mounted in Mowiol.

Myoblast transfection and differentiation

Immortalized (p53 negative) mouse myoblasts (Gregor et al., 2006) were cultivated on collagen-coated (5 mg/ml in PBS overnight; Sigma-Aldrich) tissue culture dishes in F-10 (Invitrogen) medium containing 20% FCS, 2.5 ng/ml human basic FGF (Promega), 100 U/ml penicillin, and 100 μg/ml streptomycin. Myoblasts were transfected using FuGENE6 (Roche), and differentiation was initiated after 12–16 h by switching the medium to DME containing 5% horse serum, 100 U/ml penicillin, and 100 μg/ml streptomycin. After 4–6 d, myotubes were fixed with chilled (−20°C) methanol and processed for immunolabeling and subsequent laser-scanning confocal microscopy. For IB analysis of protein expression profiles during differentiation, myoblast cultures were differentiated, and cells were lysed directly in reducing SDS sample buffer at different time points.

Fluorescence microscopy and imaging

Immunolabeled tissue and cell samples mounted in Mowiol were viewed in a fluorescence microscope (Axiophot; Carl Zeiss MicroImaging, Inc.) using plan Neofluar 40× NA 1.2 (for tissue sections; Carl Zeiss MicroImaging, Inc.) and plan Apochromat 63× NA 1.3 (for cells and teased fibers; Carl Zeiss MicroImaging, Inc.) objectives. Confocal images were recorded using the LSM510 module (Carl Zeiss MicroImaging, Inc.) and the LSM510 software package (version 3.2 SP2; Carl Zeiss MicroImaging, Inc.). Images were processed using LSM Image Browser (generation of projections of confocal stacks; gamma/contrast adjustments; version 3.2; Carl Zeiss MicroImaging, Inc.) and Photoshop CS2 (cropping and splitting of color channels; Adobe) and were mounted/labeled using Illustrator CS2 (Adobe).

EM

For preembedding immuno-EM, perfusion-fixed (2% PFA in PBS) adult rat EDL was dissected and teased into small fiber bundles before shock freezing in liquid nitrogen–cooled isopentane. Samples were thawed in PBS, treated with 0.2% Triton X-100 in PBS for 1 h, and blocked for 1 h in 0.1% Triton X-100, 0.1% BSA, and 1:25 normal goat serum in PBS (blocking solution). For primary immunolabeling, teased fibers were incubated

overnight at 4°C in a mixture of mAb 7A8 to plectin and antiserum #1710 to βDG (diluted in blocking solution without serum). After washing for 1 h (0.2% BSA in PBS), samples were incubated overnight at 4°C in a mixture of gold-conjugated goat anti–mouse (5 nm) and goat anti–rabbit (10 nm) secondary antibodies (British Biocell International). Gold-labeled fibers were washed in PBS, postfixed in 2.5% glutaraldehyde for 30 min, and washed in double-distilled water before silver enhancement for 1 h (R-GENT SE-EM kit; Aurion). Samples were immersed in 0.5% OsO_4 in PBS for 15 min, dehydrated, and embedded in epoxy resin (agar 100; Agar Scientific Ltd.). Thin sections were cut with an ultramicrotome (Ultracut S; Leica), mounted on copper grids, counterstained with uranyl acetate and lead citrate, and examined at 80 kV in an electron microscope (JEM-1210; JEOL). Digital images were acquired and processed using a camera (Morada; Olympus) and the analySIS software package (Olympus).

Preparation of total muscle lysates and microsome fractions

Hind leg muscles were dissected from C57BL/10 control and *mdx* mice, snap frozen in liquid nitrogen, and ground in a mortar. Muscles were homogenized in solution A (20 mM $Na_4P_2O_7$, 20 mM Na-PO_4, pH 7.4, 0.303 M sucrose, 0.5 mM EDTA, 1 mM $MgCl_2$, 2 mM PMSF, and Complete mini protease inhibitor cocktail [Roche]) using a Dounce homogenizer (~10 strokes). Part of the crude homogenate (total muscle lysate) was mixed with an equal volume of SDS sample buffer (0.4 M Tris, pH 6.8, 0.5 M DTT, 10% SDS, 50% glycerol, and 0.1% bromophenol blue) for further analysis; the rest was centrifuged for 15 min at 20,000 *g*, and the pellet was rehomogenized. Combined supernatants were filtered through six layers of cheesecloth and centrifuged for 15 min at 25,000 *g*. The pellet was discarded. To the supernatant, solid KCl was added to a final concentration of 0.6 M. After centrifugation for 35 min at 200,000 *g*, the pellet was resuspended in solution B (20 mM Tris-maleate, pH 7.4, 0.303 M sucrose, 0.6 M KCl, and the same protease inhibitors as in solution A). After incubating for 1 h, KCl-washed microsomes were pelleted for 35 min at 200,000 *g* and resuspended in solution B without KCl. 5 g of muscle yielded 0.5 ml of microsome suspension. All steps were performed at 4°C on ice. For subsequent IB analysis, microsome suspensions were mixed with 5 vol SDS sample buffer.

Gel electrophoresis and IB

Proteins were separated using standard 5 or 15% SDS-PAGE. Note the considerably higher concentration of SDS (~60 mg/ml) in our samples compared with standard conditions (~20 mg/ml). Under these conditions, immunoblot analysis of microsome fractions generally gave much better results, which are likely caused by the enhanced solubilization of membrane-associated protein complexes in these lipid-rich fractions. For IB, proteins were transferred to nitrocellulose membranes, and membranes were blocked with 5% nonfat dried milk in PBS–0.05% Tween 20 and incubated with primary and AP-conjugated secondary antibodies. For quantitation, stained membranes were scanned, and bands were evaluated using the ImageQuant 5.1 software package (Molecular Dynamics). Normalization factors based on total protein content or tubulin signals were applied to the values measured.

Co-IP

Mouse myoblasts (Gregor et al., 2006), mouse keratinocytes (Andrä et al., 2003), and CaCo-2 (HTB-37; American Type Culture Collection) were cultured as recommended or described previously. IP with antisera to plectin and βDG was performed essentially as described previously (James et al., 2000). In brief, clarified cell extracts in RIPA buffer were incubated for 2 h at 4°C with antibodies or, for control experiments, without antibodies or with host sera. Immunocomplexes were collected by centrifugation after a further 1-h incubation with protein A– or G–Sepharose beads (GE Healthcare) and extensive washing with RIPA buffer and were subsequently analyzed by IB. For IP from muscle tissue, total muscle lysates were prepared as for microsome preparations with the addition of 0.5% Triton X-100 to solution A. Part of the lysates was mixed with SDS sample buffer (total lysates), and the rest was incubated for 3 h with protein A–Sepharose beads and centrifuged (IP lysates) before incubation with antibodies overnight. Immunocomplexes were captured by protein A–Sepharose beads and eluted with SDS sample buffer.

Expression and purification of protein fragments

Recombinant protein fragments were expressed in *Escherichia coli* BL21(DE3) and purified as described previously (Rezniczek et al., 2004).

Blot overlay assay

Protein fragments were transferred to nitrocellulose membranes after 10% SDS-PAGE. Membranes were blocked with 5% BSA in TBS containing 0.5% Tween 20 and overlaid with 10 μg/ml of proteins in 20 mM Hepes, pH 7.5, 150 mM NaCl, 2 mM $MgCl_2$, 1 mM DTT, and 5% BSA and incubated overnight at 4°C with agitation. Bound proteins were detected by IB using protein- or epitope tag–specific primary and HRP-conjugated secondary antibodies or (in the case of His- and S-tagged fragments) by using the India HIS detection system (Pierce Chemical Co.) and HRP-conjugated S protein (Novagen), respectively.

Microtiter plate–binding assay

The experimental details of this binding assay have been described previously (Rezniczek et al., 2004). In brief, proteins immobilized on microtiter plates were overlaid with Eu^{3+}-labeled proteins in solution at different concentrations. After washing, the amounts of proteins bound were determined by measuring Eu^{3+} fluorescence in comparison with a standard.

Online supplemental material

Fig. S1 shows the binding data (blot overlay assays) summarized in the table in Fig. 4 B as well as additional microtiter plate–binding data. Fig. S2 shows immunofluorescence images of tissue sections from wild-type and *mdx*/utr$^{-/-}$ mice coimmunolabeled with antibodies to plectin and βDG as well as immunoblots of wild-type and *mdx*/utr$^{-/-}$ muscle lysates using primary antibodies to plectin, dystrophin, utrophin, and βDG. Online supplemental material is available at http://www.jcb.org/cgi/content/full/jcb.200604179/DC1.

We thank U. Mayer for providing antibodies to integrin α7B.

This work was supported by the Austrian Science Research Fund grant P17862-B09 (to G. Wiche) and the Wellcome Trust Research Career Development award 042180 (to S.J. Winder).

Submitted: 28 April 2006
Accepted: 16 February 2007

References

Abrahamsberg, C., P. Fuchs, S. Osmanagic-Myers, I. Fischer, F. Propst, A. Elbe-Bürger, and G. Wiche. 2005. Targeted ablation of plectin isoform 1 uncovers role of cytolinker proteins in leukocyte recruitment. *Proc. Natl. Acad. Sci. USA*. 102:18449–18454.

Andrä, K., H. Lassmann, R. Bittner, S. Shorny, R. Fässler, F. Propst, and G. Wiche. 1997. Targeted inactivation of plectin reveals essential function in maintaining the integrity of skin, muscle, and heart cytoarchitecture. *Genes Dev.* 11:3143–3156.

Andrä, K., B. Nikolic, M. Stöcher, D. Drenckhahn, and G. Wiche. 1998. Not just scaffolding: plectin regulates actin dynamics in cultured cells. *Genes Dev.* 12:3442–3451.

Andrä, K., I. Kornacker, A. Jörgl, M. Zörer, D. Spazierer, P. Fuchs, I. Fischer, and G. Wiche. 2003. Plectin-isoform-specific rescue of hemidesmosomal defects in plectin (−/−) keratinocytes. *J. Invest. Dermatol.* 120:189–197.

Bellin, R.M., T.W. Huiatt, D.R. Critchley, and R.M. Robson. 2001. Synemin may function to directly link muscle cell intermediate filaments to both myofibrillar Z-lines and costameres. *J. Biol. Chem.* 276:32330–32337.

Blake, D.J., and E. Martin-Rendon. 2002. Intermediate filaments and the function of the dystrophin-protein complex. *Trends Cardiovasc. Med.* 12:224–228.

Bloch, R.J., Y. Capetanaki, A. O'Neill, P. Reed, M.W. Williams, W.G. Resneck, N.C. Porter, and J.A. Ursitti. 2002. Costameres: repeating structures at the sarcolemma of skeletal muscle. *Clin. Orthop. Relat. Res.* 403: S203–S210.

Burton, E.A., and K.E. Davies. 2002. Muscular dystrophy–reason for optimism? *Cell*. 108:5–8.

Capetanaki, Y. 2002. Desmin cytoskeleton: a potential regulator of muscle mitochondrial behavior and function. *Trends Cardiovasc. Med.* 12:339–348.

Cluchague, N., C. Moreau, C. Rocher, S. Pottier, G. Leray, Y. Cherel, and E. Le Rumeur. 2004. beta-Dystroglycan can be revealed in microsomes from mdx mouse muscle by detergent treatment. *FEBS Lett.* 572:216–220.

Cohn, R.D., U. Mayer, G. Saher, R. Herrmann, A. van der Flier, A. Sonnenberg, L. Sorokin, and T. Voit. 1999. Secondary reduction of alpha7B integrin in laminin alpha2 deficient congenital muscular dystrophy supports an additional transmembrane link in skeletal muscle. *J. Neurol. Sci.* 163:140–152.

Cox, G.A., Y. Sunada, K.P. Campbell, and J.S. Chamberlain. 1994. Dp71 can restore the dystrophin-associated glycoprotein complex in muscle but fails to prevent dystrophy. *Nat. Genet.* 8:333–339.

Ervasti, J.M. 2003. Costameres: the Achilles' heel of Herculean muscle. *J. Biol. Chem.* 278:13591–13594.

Fuchs, P., M. Zörer, G.A. Rezniczek, D. Spazierer, S. Oehler, M.J. Castanon, R. Hauptmann, and G. Wiche. 1999. Unusual 5′ transcript complexity of plectin isoforms: novel tissue-specific exons modulate actin binding activity. *Hum. Mol. Genet.* 8:2461–2472.

Geerts, D., L. Fontao, M.G. Nievers, R.Q. Schaapveld, P.E. Purkis, G.N. Wheeler, E.B. Lane, I.M. Leigh, and A. Sonnenberg. 1999. Binding of integrin α6β4 to plectin prevents plectin association with F-actin but does not interfere with intermediate filament binding. *J. Cell Biol.* 147:417–434.

Greenberg, D.S., Y. Sunada, K.P. Campbell, D. Yaffe, and U. Nudel. 1994. Exogenous Dp71 restores the levels of dystrophin associated proteins but does not alleviate muscle damage in mdx mice. *Nat. Genet.* 8:340–344.

Gregor, M., A. Zeöld, S. Oehler, K. Andrä, P. Marobela, G. Fuchs, H.D.G. Weigel, and G. Wiche. 2006. Plectin scaffolds recruit energy-controlling AMP-activated protein kinase (AMPK) in differentiated myofibers. *J. Cell Sci.* 119:1864–1875.

Hijikata, T., T. Murakami, H. Ishikawa, and H. Yorifuji. 2003. Plectin tethers desmin intermediate filaments onto subsarcolemmal dense plaques containing dystrophin and vinculin. *Histochem. Cell Biol.* 119:109–123.

Hnia, K., D. Zouiten, S. Cantel, D. Chazalette, G. Hugon, J.A. Fehrentz, A. Masmoudi, A. Diment, J. Bramham, D. Mornet, and S.J. Winder. 2007. ZZ domain of dystrophin and utrophin: topology and mapping of a beta-dystroglycan interaction site. *Biochem. J.* 401:667–677.

Ibraghimov-Beskrovnaya, O., J.M. Ervasti, C.J. Leveille, C.A. Slaughter, S.W. Sernett, and K.P. Campbell. 1992. Primary structure of dystrophin-associated glycoproteins linking dystrophin to the extracellular matrix. *Nature*. 355:696–702.

Ilsley, J.L., M. Sudol, and S.J. Winder. 2001. The interaction of dystrophin with beta-dystroglycan is regulated by tyrosine phosphorylation. *Cell. Signal.* 13:625–632.

Ilsley, J.L., M. Sudol, and S.J. Winder. 2002. The WW domain: linking cell signalling to the membrane cytoskeleton. *Cell. Signal.* 14:183–189.

James, M., A. Nuttall, J.L. Ilsley, K. Ottersbach, J.M. Tinsley, M. Sudol, and S.J. Winder. 2000. Adhesion-dependent tyrosine phosphorylation of (beta)-dystroglycan regulates its interaction with utrophin. *J. Cell Sci.* 113:1717–1726.

Lunter, P.C., and G. Wiche. 2002. Direct binding of plectin to Fer kinase and negative regulation of its catalytic activity. *Biochem. Biophys. Res. Commun.* 296:904–910.

Newey, S.E., E.V. Howman, C.P. Ponting, M.A. Benson, R. Nawrotzki, N.Y. Loh, K.E. Davies, and D.J. Blake. 2001. Syncoilin, a novel member of the intermediate filament superfamily that interacts with alpha-dystrobrevin in skeletal muscle. *J. Biol. Chem.* 276:6645–6655.

Nikolic, B., E. Mac Nulty, B. Mir, and G. Wiche. 1996. Basic amino acid residue cluster within nuclear targeting sequence motif is essential for cytoplasmic plectin-vimentin network junctions. *J. Cell Biol.* 134:1455–1467.

Ohlendieck, K., and K.P. Campbell. 1991. Dystrophin-associated proteins are greatly reduced in skeletal muscle from mdx mice. *J. Cell Biol.* 115:1685–1694.

Osmanagic-Myers, S., and G. Wiche. 2004. Plectin-RACK1 (receptor for activated C kinase 1) scaffolding: a novel mechanism to regulate protein kinase C activity. *J. Biol. Chem.* 279:18701–18710.

Paulin, D., and Z. Li. 2004. Desmin: a major intermediate filament protein essential for the structural integrity and function of muscle. *Exp. Cell Res.* 301:1–7.

Pfendner, E., F. Rouan, and J. Uitto. 2005. Progress in epidermolysis bullosa: the phenotypic spectrum of plectin mutations. *Exp. Dermatol.* 14:241–249.

Poon, E., E.V. Howman, S.E. Newey, and K.E. Davies. 2002. Association of syncoilin and desmin: linking intermediate filament proteins to the dystrophin-associated protein complex. *J. Biol. Chem.* 277:3433–3439.

Reipert, S., F. Steinböck, I. Fischer, R.E. Bittner, A. Zeöld, and G. Wiche. 1999. Association of mitochondria with plectin and desmin intermediate filaments in striated muscle. *Exp. Cell Res.* 252:479–491.

Rezniczek, G.A., J.M. de Pereda, S. Reipert, and G. Wiche. 1998. Linking integrin α6β4-based cell adhesion to the intermediate filament cytoskeleton: direct interaction between the beta4 subunit and plectin at multiple molecular sites. *J. Cell Biol.* 141:209–225.

Rezniczek, G.A., C. Abrahamsberg, P. Fuchs, D. Spazierer, and G. Wiche. 2003. Plectin 5′-transcript diversity: short alternative sequences determine stability of gene products, initiation of translation and subcellular localization of isoforms. *Hum. Mol. Genet.* 12:3181–3194.

Rezniczek, G.A., L. Janda, and G. Wiche. 2004. Plectin. *Methods Cell Biol.* 78:721–755.

Rouger, K., M. Le Cunff, M. Steenman, M.C. Potier, N. Gibelin, C.A. Dechesne, and J.J. Leger. 2002. Global/temporal gene expression in diaphragm and hindlimb muscles of dystrophin-deficient (mdx) mice. *Am. J. Physiol. Cell Physiol.* 283:C773–C784.

Rybakova, I.N., J.L. Humston, K.J. Sonnemann, and J.M. Ervasti. 2006. Dystrophin and utrophin bind actin through distinct modes of contact. *J. Biol. Chem.* 281:9996–10001.

Schiaffino, S., L. Gorza, S. Sartore, L. Saggin, S. Ausoni, M. Vianello, K. Gundersen, and T. Lomo. 1989. Three myosin heavy chain isoforms in type 2 skeletal muscle fibres. *J. Muscle Res. Cell Motil.* 10:197–205.

Schröder, R., R.R. Mundegar, M. Treusch, U. Schlegel, I. Blümcke, K. Owaribe, and T.M. Magin. 1997. Altered distribution of plectin/HD1 in dystrophinopathies. *Eur. J. Cell Biol.* 74:165–171.

Schröder, R., D.O. Fürst, C. Klasen, J. Reimann, H. Herrmann, and P.F. van der Ven. 2000. Association of plectin with Z-discs is a prerequisite for the formation of the intermyofibrillar desmin cytoskeleton. *Lab. Invest.* 80:455–464.

Schröder, R., D. Pacholsky, J. Reimann, J. Matten, G. Wiche, D.O. Fürst, and P.F. van der Ven. 2002. Primary longitudinal adhesion structures: plectin-containing precursors of costameres in differentiating human skeletal muscle cells. *Histochem. Cell Biol.* 118:301–310.

Sevcik, J., L. Urbanikova, J. Kost'an, L. Janda, and G. Wiche. 2004. Actin-binding domain of mouse plectin. Crystal structure and binding to vimentin. *Eur. J. Biochem.* 271:1873–1884.

Spence, H.J., Y.J. Chen, and S.J. Winder. 2002. Muscular dystrophies, the cytoskeleton and cell adhesion. *Bioessays*. 24:542–552.

Steinböck, F.A., B. Nikolic, P.A. Coulombe, E. Fuchs, P. Traub, and G. Wiche. 2000. Dose-dependent linkage, assembly inhibition and disassembly of vimentin and cytokeratin 5/14 filaments through plectin's intermediate filament-binding domain. *J. Cell Sci.* 113:483–491.

Stone, M.R., A. O'Neill, D. Catino, and R.J. Bloch. 2005. Specific interaction of the actin-binding domain of dystrophin with intermediate filaments containing keratin 19. *Mol. Biol. Cell.* 16:4280–4293.

Tinsley, J., N. Deconinck, R. Fisher, D. Kahn, S. Phelps, J.M. Gillis, and K. Davies. 1998. Expression of full-length utrophin prevents muscular dystrophy in mdx mice. *Nat. Med.* 4:1441–1444.

Wiche, G., R. Krepler, U. Artlieb, R. Pytela, and H. Denk. 1983. Occurrence and immunolocalization of plectin in tissues. *J. Cell Biol.* 97:887–901.

Wilhelmsen, K., S.H. Litjens, I. Kuikman, N. Tshimbalanga, H. Janssen, I. van den Bout, K. Raymond, and A. Sonnenberg. 2005. Nesprin-3, a novel outer nuclear membrane protein, associates with the cytoskeletal linker protein plectin. *J. Cell Biol.* 171:799–810.

Yurchenco, P.D., Y.S. Cheng, K. Campbell, and S. Li. 2004. Loss of basement membrane, receptor and cytoskeletal lattices in a laminin-deficient muscular dystrophy. *J. Cell Sci.* 117:735–742.